HNNLO: a Monte Carlo program to compute Higgs boson production at hadron colliders

Stefano Catani,   Massimiliano Grazzini[∗]

INFN, Sezione di Firenze, Via Sansone 1, I-50019 Sesto Fiorentino, Florence, Italy

We consider Higgs boson production through gluon–gluon fusion in hadron collisions. We present a numerical program that computes the cross section up to NNLO in QCD perturbation theory. The program includes the decay modes $H \rightarrow \gamma\gamma$, $H \rightarrow WW \rightarrow l\nu l\nu$, $H \rightarrow ZZ \rightarrow 4$ leptons, and allows the user to apply arbitrary cuts on the momenta of the partons and of the photons or leptons that are produced in the final state.

[∗]Speaker.

1. INTRODUCTION

Gluon-gluon fusion is the main production channel of the Standard Model Higgs boson at the LHC. At leading order (LO) in QCD perturbation theory, the cross section is proportional to α_S^2, α_S being the QCD coupling. The QCD radiative corrections to the total cross section are known at the next-to-leading order (NLO) [1, 2, 3] and at the next-to-next-to-leading order (NNLO) [4, 5, 6, 7, 8, 9]. The effects of a jet veto on the total cross section has been studied up to NNLO [10]. We recall that all the results at NNLO have been obtained by using the large-M_t approximation, M_t being the mass of the top quark.

These NNLO calculations can be supplemented with soft-gluon resummed calculations at next-to-next-to-leading logarithmic (NNLL) accuracy either to improve the quantitative accuracy of the perturbative predictions (as in the case of the total cross section [11, 12]) or to provide reliable predictions in phase-space regions where fixed-order calculations are known to fail (as in the case of the q_T distribution of the Higgs boson [13, 14, 15] at small q_T).

A common feature of these NNLO and NNLL calculations is that they are fully inclusive over the produced final state (in particular, over final-state QCD radiation). Therefore they refer to situations where the experimental cuts are either ignored (as in the case of the total cross section) or taken into account only in simplified cases (as in the case of the jet vetoed cross section). The impact of higher-order corrections may be strongly dependent on the details of the applied cuts and also the shape of various distributions is typically affected by these details.

The first NNLO calculation that fully takes into account experimental cuts was reported in Ref. [16], considering the decay mode $H \rightarrow \gamma\gamma$ (see also [17]). In Ref. [18] the calculation is extended to the decay mode $H \rightarrow WW \rightarrow l\nu l\nu$ (see also [19]).

In Ref. [20] we have proposed a method to perform NNLO calculations and we have applied it to perform an independent computation of the Higgs production cross section. The method is completely different from that used in Refs. [16, 18]. Our calculation is implemented in a fully-exclusive parton level event generator. This feature makes it particularly suitable for practical applications to the computation of distributions in the form of bin histograms. Our numerical program can be downloaded from [21]. The decay modes that are currently implemented are $H \rightarrow \gamma\gamma$ [20], $H \rightarrow WW \rightarrow l\nu l\nu$ and $H \rightarrow ZZ \rightarrow 4$ leptons [22].

In the following we present a brief selection of results that can be obtained by our program. We consider Higgs boson production at the LHC and use the MRST2004 parton distributions [23], with parton densities and α_S evaluated at each corresponding order (i.e., we use $(n+1)$-loop α_S at N^{n}LO, with $n = 0, 1, 2$). The renormalization and factorization scales are fixed to the value $\mu_R = \mu_F = M_H$, where M_H is the mass of the Higgs boson.

2. RESULTS FOR THE DECAY MODE $H \rightarrow \gamma\gamma$

We consider the production of a Higgs boson of mass $M_H = 125$ GeV in the $H \rightarrow \gamma\gamma$ decay mode and follow Ref. [24] to apply cuts on the photons. For each event, we classify the photon transverse momenta according to their minimum and maximum value, $p_{T\min}$ and $p_{T\max}$. The photons are required to be in the central rapidity region, $|\eta| < 2.5$, with $p_{T\min} > 35$ GeV and $p_{T\max} > 40$ GeV. We also require the photons to be isolated: the hadronic (partonic) transverse
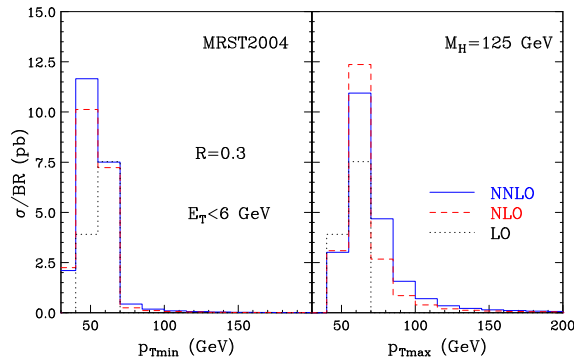
Figure 1: Distributions in $p_{T\min}$ and $p_{T\max}$ for the diphoton signal at the LHC. The cross section is divided by the branching ratio in two photons.

energy in a cone of radius $R = 0.3$ along the photon direction has to be smaller than 6 GeV. Using these cuts the impact of the NNLO corrections on the NLO total cross section is reduced from 19% to 11%.

In Fig. 1 we plot the distributions in $p_{T\min}$ and $p_{T\max}$ of the signal process $gg \rightarrow H \rightarrow \gamma\gamma$. We note that the shape of these distributions sizeably differs when going from LO to NLO and to NNLO. The origin of these perturbative instabilities is well known [25]. Since the LO spectra are kinematically bounded by $p_T \leq M_H/2$, each higher-order perturbative contribution produces (integrable) logarithmic singularities in the vicinity of that boundary. More detailed studies are necessary to assess the theoretical uncertainties of these fixed-order results and the relevance of all-order resummed calculations.

In Fig. 2 we consider the (normalized) distribution in the variable $\cos\theta^*$, where θ^* is the polar angle of one of the photons in the rest frame of the Higgs boson [1]. At small values of $\cos\theta^*$ the distribution is quite stable with respect to higher order QCD corrections. We also note that the LO distribution vanishes beyond the value $\cos\theta^*_{\max} < 1$. The upper bound $\cos\theta^*_{\max}$ is due to the fact that the photons are required to have a minimum p_T of 35 GeV. As in the case of Fig. 1, in the vicinity of this LO kinematical boundary there is an instability of the perturbative results beyond LO.

3. RESULTS FOR THE DECAY MODE $H \rightarrow l\nu l\nu$

We now consider the production of a Higgs boson with mass $M_H = 165$ GeV in the decay mode $H \rightarrow l\nu l\nu$. We apply a set of *preselection* cuts taken from the study of Ref. [26]. The charged leptons have p_T larger than 20 GeV, and $|\eta| < 2$. The missing p_T is larger than 20 GeV and the invariant mass of the charged leptons is smaller than 80 GeV. Finally, the azimuthal separation of the charged leptons in the transverse plane ($\Delta\phi$) is smaller than 135°. By applying these cuts the impact of the NNLO corrections on the NLO result does not change and is of about 20%.

In Fig.3 we plot the $\Delta\phi$ distribution at LO, NLO and NNLO. As is well known [27], the charged leptons from the Higgs boson signal tend to be close in angle, and thus the distribution is

---

[1]We thank Suzanne Gascon and Markus Schumacher for suggesting the use of this variable.
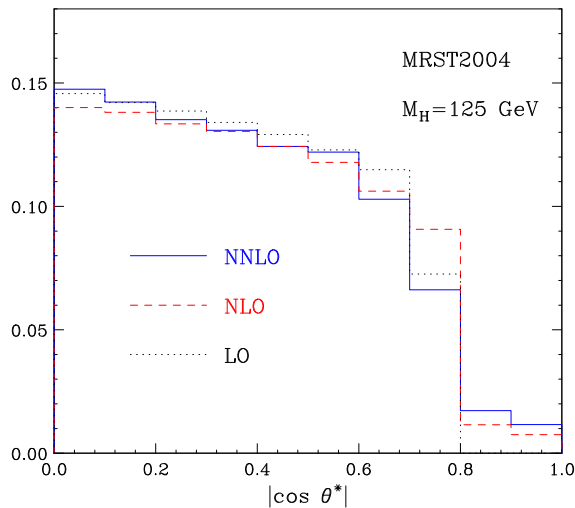
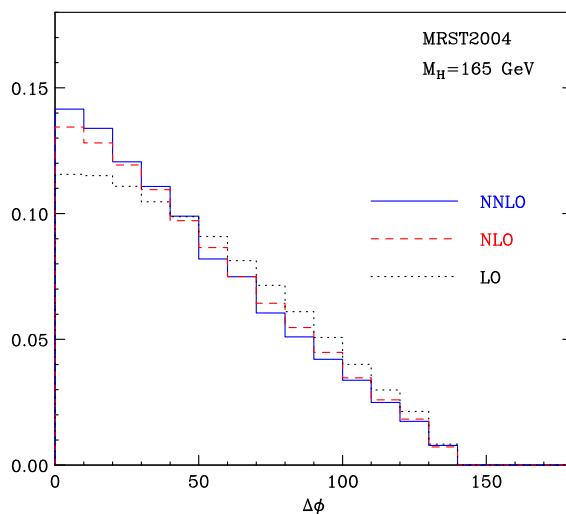**Figure 2:** Normalized distribution in the variable $\cos\theta^*$.

Figure 3: Normalized $\Delta\phi$ distribution at LO, NLO, NNLO.

peaked at small $\Delta\phi$. We note that the effect of the QCD corrections is to increase the steepness of the distribution, from LO to NLO and from NLO to NNLO.

We finally apply the set of selection cuts designed to isolate the Higgs boson signal [26]. The transverse momenta of the two charged leptons are classified according to their minimum and maximum value, $p_{T\min}$ and $p_{T\max}$. They should fulfil $p_{T\min} > 25$ GeV and 35 GeV $< p_{T\max} < 50$ GeV. The missing p_T of the event should be larger than 20 GeV and the invariant mass of the charged leptons should be smaller than 35 GeV. To exploit the steepness of the $\Delta\phi$ distribution shown in Fig. 3, $\Delta\phi$ should be smaller than 45°. Finally, there should be no jets with p_T^{jet} larger than a given value p_T^{veto}.

The corresponding cross sections, for different values of p_T^{veto}, are reported in Table 1.

4

p_T^{veto} (GeV)	σ_{NLO} (fb)	σ_{NNLO} (fb)
no veto	21.26 ± 0.05	22.21 ± 0.32
40	18.62 ± 0.05	17.38 ± 0.34
30	17.18 ± 0.05	15.74 ± 0.35
20	14.42 ± 0.05	11.31 ± 0.38

Table 1: *Cross sections for* $pp \to H + X \to WW + X \to l\nu l\nu + X$ *at the LHC when selection cuts are applied for different* p_T^{veto}.

We see that, even without the jet veto, the impact of radiative corrections is strongly reduced with this choice of cuts. The jet veto further reduces the effect of the NNLO corrections, which become negative for $p_T^{\text{veto}} \lesssim 40$ GeV.

4. SUMMARY

We have illustrated the results of a calculation of the Higgs boson production cross section at the LHC up to NNLO in QCD perturbation theory. The calculation is performed by using the numerical program HNNLO, which includes all the relevant decay modes of the Higgs boson, namely, $H \to \gamma\gamma$, $H \to WW \to l\nu l\nu$ and $H \to ZZ \to 4$ leptons. The program allows the user to apply arbitrary cuts on the momenta of the partons and of the photons/leptons produced in the final state, and to obtain the required distributions in the form of bin histograms. We have presented a brief selection of numerical results for the decay modes $H \to \gamma\gamma$ and $H \to WW \to l\nu l\nu$. More detailed results for the decay modes $H \to WW$ and $H \to ZZ$ can be found in Ref. [22]. The fortran code HNNLO can be downloaded from [21].

References

[1] S. Dawson, Nucl. Phys. B359 (1991) 283.

[2] A. Djouadi, M. Spira and P.M. Zerwas, Phys. Lett. B264 (1991) 440.

[3] M. Spira et al., Nucl. Phys. B453 (1995) 17, hep-ph/9504378.

[4] R.V. Harlander, Phys. Lett. B492 (2000) 74, hep-ph/0007289.

[5] S. Catani, D. de Florian and M. Grazzini, JHEP 05 (2001) 025, hep-ph/0102227.

[6] R.V. Harlander and W.B. Kilgore, Phys. Rev. D64 (2001) 013015, hep-ph/0102241.

[7] R.V. Harlander and W.B. Kilgore, Phys. Rev. Lett. 88 (2002) 201801, hep-ph/0201206.

[8] C. Anastasiou and K. Melnikov, Nucl. Phys. B646 (2002) 220, hep-ph/0207004.

[9] V. Ravindran, J. Smith and W.L. van Neerven, Nucl. Phys. B665 (2003) 325, hep-ph/0302135.

[10] S. Catani, D. de Florian and M. Grazzini, JHEP 01 (2002) 015, hep-ph/0111164.

[11] S. Catani et al., JHEP 07 (2003) 028, hep-ph/0306211.

[12] S. Moch and A. Vogt, Phys. Lett. B631 (2005) 48, hep-ph/0508265.

[13] G. Bozzi et al., Phys. Lett. B564 (2003) 65, hep-ph/0302104.

[14] G. Bozzi et al., Nucl. Phys. B737 (2006) 73, hep-ph/0508068.

[15] G. Bozzi et al., Nucl. Phys. B791 (2008) 1, arXiv:0705.3887 [hep-ph].

[16] C. Anastasiou, K. Melnikov and F. Petriello, Nucl. Phys. B724 (2005) 197, hep-ph/0501130.

[17] F. Stockli, A.G. Holzner and G. Dissertori, JHEP 10 (2005) 079, hep-ph/0509130.

[18] C. Anastasiou, G. Dissertori and F. Stockli, JHEP 09 (2007) 018, arXiv:0707.2373 [hep-ph].

[19] C. Anastasiou et al., arXiv:0801.2682 [hep-ph].

[20] S. Catani and M. Grazzini, Phys. Rev. Lett. 98 (2007) 222002, hep-ph/0703012.

[21] http://theory.fi.infn.it/grazzini/codes.html .

[22] M. Grazzini, arXiv:0801.3232 [hep-ph].

[23] A.D. Martin et al., Phys. Lett. B604 (2004) 61, hep-ph/0410230.

[24] CMS Physics, Technical Design Report, Vol. II Physics Performance , report CERN/LHCC 2006-021.

[25] S. Catani and B.R. Webber, JHEP 10 (1997) 005, hep-ph/9710333.

[26] G. Davatz et al., JHEP 05 (2004) 009, hep-ph/0402218.

[27] M. Dittmar and H.K. Dreiner, Phys. Rev. D55 (1997) 167, hep-ph/9608317.